Mechanical rejuvenation and overaging in the soft glassy rheology model

Mya Warren* and Jörg Rottler
Department of Physics and Astronomy, The University of British Columbia, 6224 Agricultural Road, Vancouver, BC, V6T 1Z1, Canada
(Received 4 July 2008; published 8 October 2008)

Mechanical rejuvenation and overaging of glasses is investigated through stochastic simulations of the soft glassy rheology (SGR) model. Strain- and stress-controlled deformation cycles for a wide range of loading conditions are analyzed and compared to molecular dynamics simulations of a model polymer glass. Results indicate that deformation causes predominantly rejuvenation, whereas overaging occurs only at very low temperatures, small strains, and for high initial energy states. Although the creep compliance in the SGR model exhibits full aging independent of applied load, large stresses in the nonlinear creep regime cause configurational changes leading to rejuvenation of the relaxation time spectrum probed after a stress cycle. During recovery, however, the rejuvenated state rapidly returns to the original aging trajectory due to collective relaxations of the internal strain.

DOI: 10.1103/PhysRevE.78.041502 PACS number(s): 83.50.−v, 81.05.Kf, 61.43.−j

I. INTRODUCTION

The mechanical properties of glassy materials continuously evolve due to slow, non-equilibrium dynamics, a phenomenon called physical aging [1–3]. As a consequence, the response of glasses to an applied load depends not only on measurement time t, but also on the wait time t_w that has elapsed since the glass was formed. In general, increasing wait time makes glasses less compliant and increases their resistance to plastic flow [2–14]. For glasses formed through a rapid quench from the liquid state, the effects of aging take a particularly simple form: response functions such as the creep compliance obey a self similar scaling with the wait time and depend only on the ratio t/t_w^{μ}. The aging exponent μ has been found to be approximately unity for a wide range of structural glasses moderately below the glass transition temperature [2,15].

However, large mechanical deformation and plastic yielding can modify the aging dynamics. A primary example of this phenomenon is the observed reduction in the aging exponent obtained through creep measurements of glassy polymers at large stress. Since the relaxation times of the deformed glass resemble those of a younger glass, it was hypothesized that the glass had been "rejuvenated" by the stress [2]. Experiments on a wide variety of materials including polymer glasses [6,16,17], colloidal glasses [4,5], and even the cytoskeleton of the cell [18] have shown a similar decrease in relaxation times under high loads. However, the interpretation of these results in terms of rejuvenation remains controversial. Detailed experiments by McKenna have shown that the time to equilibration of mechanically rejuvenated glasses remains essentially unchanged by the application of external load [7], suggesting that stress does not in fact change the extent of aging. Other studies indicate that the apparent enhancement of particle mobility eventually disappears after unloading [6,17], and that the configurational states of mechanically rejuvenated glasses are distinct from the states visited by aging in the absence of load [10,12,19].

Signatures of overaging due to deformation have recently been observed as well. For instance, polymer glasses subject to a stress relaxation experiment well below the glass transition temperature exhibit rapid densification for certain strains [20]. Molecular simulations of simple structural glasses show that a small amplitude strain cycle at zero temperature can decrease the inherent structure energy [10]. Also, detailed experiments by Lequeux and co-workers show overaging in systems of dense colloids, which are effectively athermal glasses. They observe changes to the entire spectrum of relaxation times [8,9]: after a period of small amplitude oscillatory shear, the glass appears rejuvenated over small time scales, and overaged over longer time scales.

The emerging picture of the phenomenology of glasses under load presents some interesting questions that seem to defy a simple explanation in terms of the rejuvenation hypothesis. First, under what loading conditions do overaging and rejuvenation occur? So far, overaging has been seen only under very specific circumstances: low temperature, small strains, and strain-controlled loading conditions. Rejuvenation, on the other hand, has been observed much more generally in deformed samples, but has been studied most extensively at high temperatures (only moderately below the glass transition temperature) and constant stress conditions. Another important question is presented by the work of McKenna [7]. What is the nature of the states created by loading, and how do we reconcile the rejuvenated relaxation spectrum with the fact that the time to equilibration is unchanged by the stress?

A comprehensive molecular model that describes aging and deformation in glasses is not available to date. However, phenomenological energy landscape approaches such as the soft glassy rheology (SGR) model [21] have been able to capture many aspects of the rheology of glasses, and have successfully been used to interpret overaging in strain-controlled experiments at low temperature [9,19]. In this study, we will use the SGR model to systematically explore the loading phase diagram in order to better understand the generality and the implications of mechanical rejuvenation and over-aging, as well as the relationship between configurational and dynamical changes. We perform stochastic simulations of the SGR model over a wide range of experi-

*mya@phas.ubc.ca

mental conditions and compare the results to molecular dynamics simulations of a model polymer glass in selected cases.

II. MODELS

A. Soft glassy rheology model

It has been found experimentally and through molecular simulations that the structural relaxation events which result in aging and plastic deformation involve the cooperative motion of groups of approximately 10–30 particles [22–24]. The premise of the SGR model is that each of these mesoscopic rearranging domains can be described by a single fictive particle in a rough free-energy landscape. This particle performs thermally or mechanically activated hops between locally harmonic "traps" in the landscape. The density of states of the traps is

$$\rho(E) = \frac{1}{x_g} \exp(-E/x_g), \quad E \geqslant 0, \tag{1}$$

where x_g is the glass transition temperature and E is the depth of a trap. At low temperature, many traps will be very long lived.

The master equation governing the dynamics of the fictive particles is [21]

$$\dot{P}(E,l,t) = -\dot{\gamma}\frac{\partial P}{\partial l} - P\Gamma_0 \exp\left[-\left(E - \frac{kl^2}{2}\right) \Big/ x\right] + \Gamma(t)\rho(E)\delta(l). \tag{2}$$

$P(E,l,t)$ is the occupation probability of a state with energy E and local strain l at time t. The energy barrier for particle hopping is reduced by the local strain energy, $E_b = E - kl^2/2$, where k is the stiffness of the well. All of the barriers have a common energy of zero, so the energy of the fictive particle in the trap is $-E_b$. On the right-hand side of Eq. (2), the first term describes the elastic motion of the fictive particles in their wells under strain rate $\dot{\gamma}$. In the absence of particle hopping, this term simply increases the local strain variable of the particles. The second term in Eq. (2) describes activated hopping out of the wells, which can be viewed as a local plastic yield event; Γ_0 is the attempt rate and x is a "noise temperature" [21]. The noise temperature is generally higher than the thermodynamic temperature, as it incorporates the effect of nonequilibrium fluctuations in the aging glass. The third term describes the transition to the new state after hopping, whose energy is chosen randomly from the density of states $\rho(E)$ and is initially unstrained; $\Gamma(t)$ is the total hopping rate at time t. The macroscopic stress in this formulation is

$$\sigma = k\langle l \rangle. \tag{3}$$

We solve the master equation (2) numerically using Monte Carlo simulations. In this work, x_g, Γ_0, and k are chosen to be 1, which has the effect of setting the units of energy, time, and strain. Note that a strain of one in these units is the average yield strain of a particle. To begin, an ensemble of ten thousand particles is initialized with trap energies chosen randomly from the equilibrium Boltzmann distribution at liquid temperature $x_l > x_g$: $P(E) = \rho(E)\exp(-E/x_l)$. The trajectories of the particles are then computed at a glassy temperature $x < x_g$. This is equivalent to an instantaneous quench to the glassy phase. In the absence of load, the system falls out of equilibrium at $x < x_g$ where the Boltzmann distribution is no longer normalizable and the system exhibits full aging, i.e., an aging exponent $\mu = 1$ [25].

For the strain-controlled loading protocol, each fictive particle is treated independently. The strain variable is increased at constant rate, and at each time step the particles i hop with probability $P_i = \Gamma_i dt$ where $\Gamma_i = \Gamma_0 \exp[-(E_i - kl_i^2/2)/x]$ is the hopping rate of the particle. The stress is computed from Eq. (3), where the average is taken over all particles. The stress-controlled loading protocol is somewhat more complicated because of the implicit relationship between the master equation and the stress. In this case, we use the kinetic Monte Carlo method [26] to evolve an ensemble of particles. A time step is chosen from a Poisson distribution with the global rate $\Gamma = \Sigma_i \Gamma_i$, and the particle that will hop is chosen with a probability proportional to each particle's individual hopping rate. The relaxed particle hops into a zero strain state, and the stress it was holding is redistributed uniformly among the particles in the system, i.e., the microscopic strains are increased evenly until Eq. (3) is satisfied again. If the stress is applied quickly, the strain energy may exceed the barrier for some elements. These are relaxed instantaneously and the procedure is repeated until a stable configuration is found.

B. Molecular dynamics

For qualitative comparison with a structural glass, we perform molecular dynamics (MD) simulations on a "bead-spring" polymer model [27] that has been studied extensively for its glass-forming properties. In this model, beads interact via a nonspecific van der Waals potential (Lennard-Jones), and bonds are modeled using the finitely extensible nonlinear elastic model (FENE) which acts to prevent chain crossing. The reference length-scale is a, the diameter of the bead; the energy scale, u_0, is determined by the strength of the van der Waals potential, and the time scale is $\tau_{\mathrm{LJ}} = \sqrt{ma^2/u_0}$, where m is the mass of a bead. The pressure and stress are therefore measured in units of u_0/a^3.

In these simulations, we consider 855 chains of 100 beads each in an originally cubic simulation volume with periodic boundary conditions. The polymers are first equilibrated at a liquid temperature of $1.2u_0/k_B$, and then quenched into the glassy state by decreasing the temperature at constant rate to below the glass transition temperature $T_g \approx 0.35u_0/k_B$ [28]. Deformation experiments are then performed on the glass at constant temperature by either applying a uniaxial load, or by imposing volume-conserving, uniaxial deformation at constant strain rate. This polymer model has been used frequently in studies of deformation of polymer glasses [29]. In particular, it demonstrates mechanical rejuvenation during nonlinear creep under large loads [14]. Except at very large strains where polymer entanglements become impor-

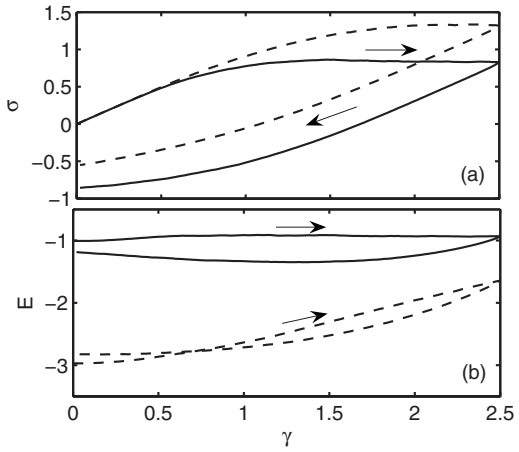

FIG. 1. (a) Stress vs strain and (b) energy vs strain at zero noise temperature. Curves are obtained from an ensemble average of 10,000 particles with initial liquid temperatures of $x_l=2$ (solid) and $x_l=1.5$ (dashed).

tant, we expect these results to be pertinent for many glassy materials.

III. RESULTS

We begin exploring the loading phase diagram in the limit of zero noise temperature and zero strain rate, where overaging has most commonly been observed. Starting configurations are created from different liquid temperatures x_l. At $x=0$, the samples are strained at constant rate to a maximum strain $\gamma_{\max}$ and then returned to zero strain at the same rate. The stress and the mean energy are plotted versus strain in Fig. 1 for two different initial liquid temperatures. Initially, the stress is linear in strain as the system responds elastically, and then becomes constant after yield. Note that the yield stress is higher for the state that was quenched from the lower liquid temperature. Also, the energy of the higher x_l configuration is lowered by the strain cycle (overaging), whereas the lower x_l configuration has a higher energy after the same cycle (rejuvenation). These results are qualitatively similar to molecular simulation results of a binary Lennard-Jones glass at zero temperature reported in Ref. [10] and appear to be generic to rough energy landscapes with many metastable states [19].

In Fig. 2, we explore in detail the effects of the noise temperature x, the initial configuration temperature x_l, and the strain rate $\dot{\gamma}$ in the strain controlled protocol described above. Here we treat x as a free adjustable parameter, although in the SGR model it is envisioned to be related to the dissipated energy of yielding elements. For each thermomechanical history, we compare the final energy after the strain cycle E_f to the energy E_0 of the same sample if it had not been strained, but simply aged at constant temperature for an equivalent amount of time. The relative energy difference $\Delta E/E_0$ is positive for rejuvenation, and negative for overaging.

In Fig. 2(a) the energy difference $\Delta E/E_0$ is plotted for samples with the same x_l and $\dot{\gamma}$, but various noise temperatures x. We see that overaging does indeed occur only at low noise temperatures, which may be why it has mostly been observed in low-temperature simulations and in colloids. The small x curves show a transition from overaging at low strains to rejuvenation at high strains. At very high strains (not shown) the glass yields, and all of the samples are maximally rejuvenated. As the noise temperature is increased, the magnitude of overaging and the maximum strain where it occurs both decrease. For $x>1$, the SGR model is in equilibrium and the effects of overaging and rejuvenation disappear except for weak transients.

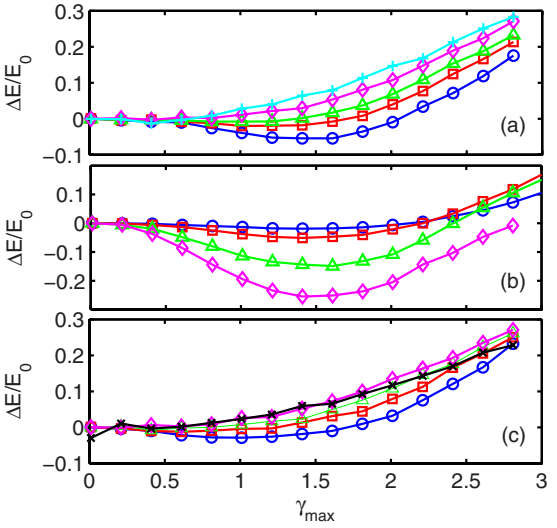

FIG. 2. (Color online) Relative difference in energy versus maximum strain after a single strain cycle of amplitude $\gamma_{\max}$. (a) Noise temperature $x=0.1$, 0.2, 0.3, 0.5, and 0.8 from bottom to top, $x_l=2$ and $\dot{\gamma}=0.25$ for each sample. (b) $x_l=1.25$, 1.5, 2.5, and 5 from top to bottom, $x=0.001$ and $\dot{\gamma}=0.25$ for each sample. (c) $\dot{\gamma}=1$ (circle), 0.5 (square), 0.25 (triangle), 0.1 (diamond), and 0.01 (cross), $x=0.5$ and $x_l=2$.

Figure 2(b) shows the energy difference at very low x for various initial states x_l. The amount of over-aging decreases as the initial energy is decreased, and asymptotically approaches zero in the case of a quench from exactly $x_l=1$. Note that the strain at which overaging is maximized does not seem to depend on the initial configuration, but always occurs at $\gamma_{\max}\approx 1.4$. Alternatively, at higher temperatures where rejuvenation is predominant, we find that the amount of rejuvenation increases with liquid temperature x_l.

Finally, the mechanical rate also plays a role in whether the energy will be reduced or increased by the strain cycle. Figure 2(c) shows relative energy changes for a sample with noise temperature $x=0.5$ for various strain rates. The amount of rejuvenation decreases with increasing strain rate for moderate strains, but the curves eventually cross as the strain approaches yield. This is due to the fact that the yield stress (or strain) increases with rate. At the highest strain rates, overaging appears possible even at high temperatures. Note, however, that high strain rates are not treated entirely realistically in this model. In the SGR model, an element yields instantaneously when strained to greater than the yield strain. However, in real solids, very fast strain rates lead to large affine displacements but relatively few plastic events as these require a finite time to relax.

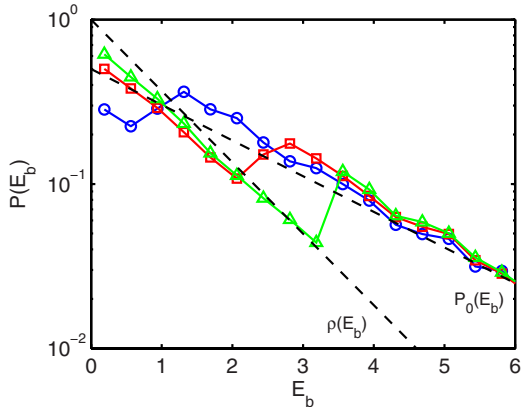

FIG. 3. (Color online) Distribution of energy barriers after a zero temperature strain cycle. $\gamma_{max}=1.5$ (circle), 2 (square), and 2.5 (triangle). The initial energy distribution $P_0(E)$ and the landscape density of states $\rho(E)$ are shown as dashed lines.

With the SGR model, further intuition can be gained by investigating the effect of mechanical deformation on the population of the traps directly. Figure 3 shows the distribution of energy barriers for various γ_{max} after a zero noise temperature strain cycle. The changes to the distribution of energy barriers due to strain at low temperature are complex and do not, in general, resemble the normal aging distribution. This was also discussed in Ref. [9] in the context of aging colloidal glasses, where it was shown that the entire spectrum of relaxation times was modified by an oscillatory shear. The strain cycle causes particles in the highest energy states (lowest barriers) to hop into new states chosen from the landscape energy distribution $\rho(E)$. Overaging, or a decrease in the mean energy of the system, then occurs when the states being relaxed are of higher energy than the mean energy of the states they hop into. At zero noise temperature, this predicts that maximum over-aging occurs at a strain amplitude γ_{max}, where $k\gamma_{max}^2/2=\int_0^\infty dE\rho(E)E=1$, or $\gamma_{max}=\sqrt{2}$. This can be seen clearly in Fig. 2(b) for all values of x_l. The strain amplitude at maximum overaging thus gives a measure of the mean energy of the landscape. The amount of overaging, or the energy at this peak strain, is due to the number of low energy states available to relax, and therefore depends sensitively on the initial configuration.

Figure 3 also helps us understand why overaging occurs primarily at low temperatures. At higher noise temperature, the high energy states that are relaxed by small strains to produce overaging are rapidly depleted via thermal activation, meaning that the peak over-aging is drastically reduced. Additionally, thermal aging results in the relaxation of lower energy states during the strain cycle, and these states are left with residual strain energy after the cycle. Consequently, the final stress increases with noise temperature, and the effective aging during the cycle is reduced.

We compare these results with molecular dynamics simulations of the model polymer glass under similar thermomechanical histories by varying the maximum strain, the strain rate, and the temperature of the glass. In order to investigate the effect of different initial states, an equilibrated liquid at $T=1.2u_0/k_B$ is quenched at different rates to the final glassy

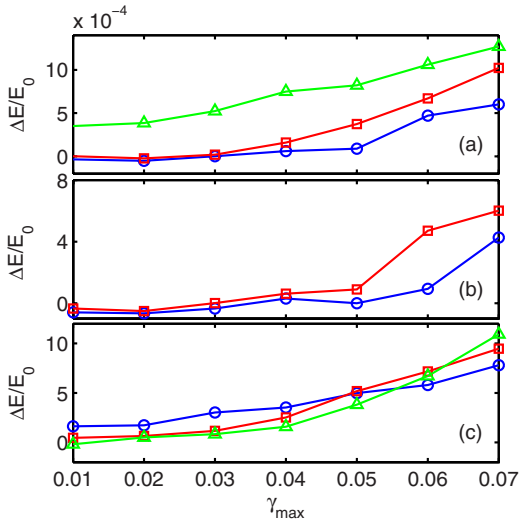

FIG. 4. (Color online) Molecular dynamics results for the relative difference in energy versus strain after a single strain cycle. (a) $T=0.01$ (circle), 0.1 (square), and $0.2u_0/k_B$ (triangle). The quench time is $t_{qu}=750\tau_{LJ}$ and $\dot{\gamma}=5.3\times10^{-5}\tau_{LJ}^{-1}$ for each sample. (b) $t_{qu}=750\tau_{LJ}$ (square) and $7500\tau_{LJ}$ (circle). $T=0.01u_0/k_B$ and $\dot{\gamma}=5.3\times10^{-5}\tau_{LJ}^{-1}$. (c) $\dot{\gamma}=5.3\times10^{-6}\tau_{LJ}^{-1}$ (circle), $5.3\times10^{-5}\tau_{LJ}^{-1}$ (square), and $5.3\times10^{-4}\tau_{LJ}^{-1}$ (triangle). $T=0.2u_0/k_B$ and $t_{qu}=750\tau_{LJ}$.

temperature. The results are shown in Fig. 4 and are qualitatively similar to behavior found in the SGR model. Figure 4(a) shows that higher temperatures lead to increased rejuvenation, Fig. 4(b) shows that initial states of higher energy (faster quench) result in more rejuvenation, and Fig. 4(c) shows increased rejuvenation at moderate strains and decreased rejuvenation at large strains as the strain rate is decreased. However, there is a significant difference between the SGR and molecular dynamics results. We have not found appreciable overaging in our molecular dynamics simulations, even at very low temperatures and fast cooling rates. This is in contrast to recent molecular dynamics results of an atomistic polymer model under a similar strain cycle [12]. The authors of this study report overaging of the simulated glass by the strain for very fast quench rates. However, this is likely because they did not compare to a non-strained control sample but to the initial (just quenched) energy before the strain cycle. We observe that even at very low temperatures, our model exhibits significant aging directly after the glass is quenched when quench rates are very high. It remains an open question to what extent overaging occurs in real polymer glasses under realistic quench and loading conditions.

Stress-controlled loading protocols similarly show rejuvenation and overaging in the SGR model. In this case, a stress step function is applied for a period of $t=10$ and then released. The change in energy due to the stress cycle is plotted in Fig. 5(a) for various noise temperatures. At low noise temperature, there is overaging at low stress and rejuvenation at high stress. At high noise temperature, there is a broad flat region for small stress, followed by a steep increase in rejuvenation at high stress within the nonlinear regime. In Fig. 5(b), the same data is plotted versus the maximum strain achieved during the stress cycle for direct comparison with the strain-controlled data. The results plotted in this way look

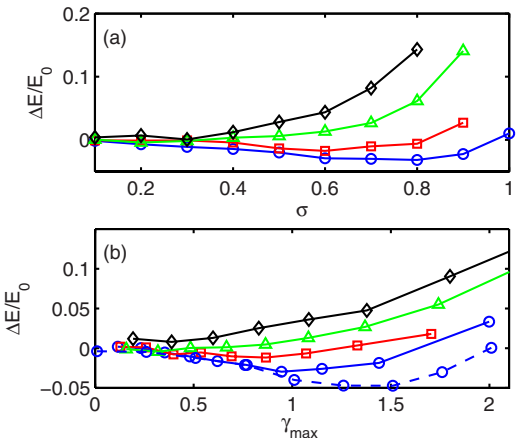

FIG. 5. (Color online) Relative energy change due to a stress cycle applied for $t=10$. In (a) the energy difference is plotted versus the stress, and in (b) the same data is plotted versus the maximum strain in the stress cycle. $x=0.1$ (circles), 0.2 (squares), 0.4 (triangles), and 0.6 (diamonds). $x_l=2$ for each sample. The dashed line in (b) is the energy versus strain for an equivalent strain-controlled protocol at $x=0.1$.

very similar to Fig. 2(a) for the strain cycle. Over-aging occurs over a similar range of noise temperature and strain, however, closer inspection shows that the amount of overaging is somewhat smaller for the stress-controlled protocol. Finishing the cycle at zero stress rather than zero strain means that low energy states that did not relax during the experiment have residual strain energy and are rejuvenated.

Our analysis so far has utilized changes in the energy of the system to identify the occurrence of rejuvenation or overaging. However, the notion of rejuvenation has its origin in an acceleration of the dynamics under load [2,4–8]. As described earlier, rejuvenation is commonly measured via a decrease in the aging exponent μ with applied stress σ. Experimentally, the aging exponent can be evaluated through creep experiments: a sample is first aged for a wait time t_w, then the creep compliance is measured as a function of time t since the stress was applied. Superposition of the creep compliance $J(t,t_w)$ of samples that have aged for different wait times reveals the t/t_w^{μ} scaling behavior. In principle, this type of analysis can also be performed in the SGR model, but is impeded by the fact that the creep compliance exhibits a clear t/t_w scaling only in the limit of $t_w \to \infty$ [30]. In particular, for quenches from a finite liquid temperature x_l, we find that the scaling regime is not accessible within a reasonable simulation time. In the creep experiments described below, we therefore initialize the trap distribution from $\rho(E)$, where the scaling regime is more easily accessible. This is equivalent to performing a quench from $x_l=\infty$. Figure 6 shows representative compliance curves for several different wait times under an applied load of $\sigma=0.75$. Indeed, compliance curves obey the t/t_w scaling behavior characteristic of trap models [25]. Interestingly, we find this scaling behavior to be independent of the magnitude of the applied stress, even within the nonlinear creep regime. Although the form of the scaling function is stress dependent [30], the decrease in the aging exponent under large load that is observed in real structural glasses does not occur in the SGR model.

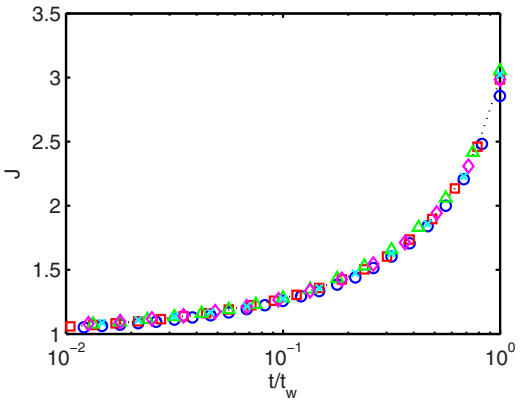

FIG. 6. (Color online) Creep compliance of the SGR model quenched from $x_l=\infty$ (see text) and aged for $t_w=100$ (circles), 316 (squares), 1000 (triangles), 3162 (diamonds), and 10 000 (×'s) at $x=0.5$ and $\sigma=0.75$ (within the nonlinear regime).

However, it is clear from the data in Fig. 5 that large stress cycles cause rejuvenation of the energy of the ensemble. To test the effect of wait time on the state of the aged samples after creep, we release the stress after a creep experiment of the same duration as the initial wait time ($t=t_w$) and measure the average energy of the unloaded system. A long creep time is chosen because, in this regime, thermal aging under stress leads to irreversible plastic deformation and maximum rejuvenation [6]. Figure 7(a) plots the energy vs wait time for four different stresses and shows that not only does the energy change nonlinearly with the stress as anticipated from Fig. 5, but the slope of the energy versus wait time curves also decreases for increasing stress. Highly stressed samples appear to have aged less.

The simple relationship between the energy and the dynamics in the SGR model implies a simultaneous change in the dynamics after the stress is released. To see this, we compute the correlation function

$$C(t,t_w) = \int_0^{\infty} dE_b P(E_b,t,t_w) e^{-(\Gamma_0 e^{-E_b/x})t} \tag{4}$$

which measures the probability that a particle in a trap at time t_w has not hopped at time t_w+t [25]. These functions are

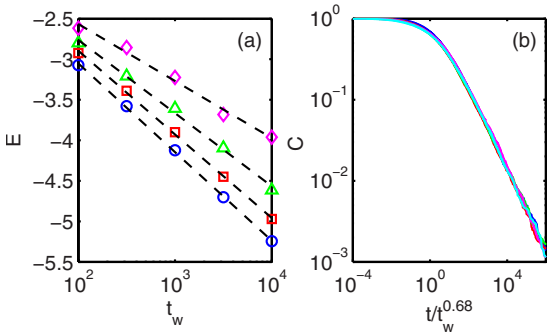

FIG. 7. (Color online) (a) Energy as a function of wait time after a stress cycle of duration $t=t_w$. $\sigma=0.05$ (circles), 0.6 (squares), 0.7 (triangles), 0.75 (diamonds). $x=0.5$ and $x_l=\infty$ for each sample. (b) Scaled correlation functions for $t_w=100$, 316, 1000, 3162, and 10 000 (all overlapping) for $\sigma=0.75$. Data collapse is obtained for $\mu=0.68$.

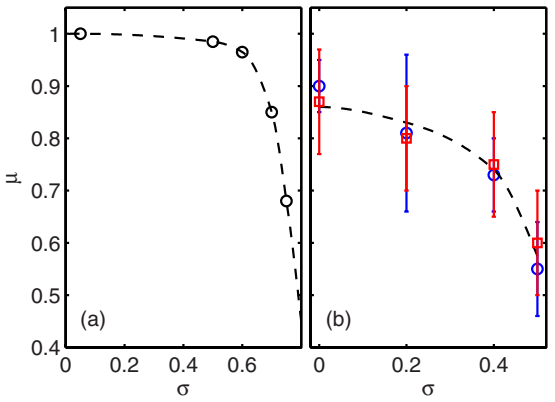

FIG. 8. (Color online) (a) Aging exponent versus the stress in the SGR model, as determined from the correlation functions (4) after a stress cycle of duration $t=t_w$. $x=0.5$ and $x_l=\infty$. (b) Aging exponent versus stress from molecular dynamics simulations of a model polymer glass using (circles) the creep compliance and (squares) the mean-squared displacement after stress release at $10t_w$. $T=0.2u_0/k_B$.

shown in Fig. 7(b) for various wait times after a nonlinear stress cycle. The shape of the correlation function is typical of glasses, although missing the initial β-relaxation decay. There is a plateau region at short times where there are very few relaxation events, followed by a rapid decrease at $t \approx t_w$. The correlation functions measured after the stress cycle perfectly superimpose with t_w; however, in contrast to the compliance curves, the scaling of the correlation functions with t_w is drastically changed by large stresses. Figure 7(b) shows that for $\sigma=0.75$, the correlation functions no longer display full aging behavior, but we find good data collapse if we rescale time with t_w^μ, where $\mu=0.68$. It appears that for stress controlled deformation at finite temperature, the relaxation time spectrum of the mechanically rejuvenated glass does indeed resemble a younger glass.

Figure 8(a) presents the variation of aging exponents with stress obtained from superposition of the correlation functions at different wait times. At small stresses, the exponent is unity, but decreases rapidly for nonlinear creep. For comparison with the polymer model, we repeat the creep experiment using molecular dynamics following a similar protocol. In MD, we extract aging exponents from superposition of mean squared displacements (see Ref. [14]) of particles after stress release. Figure 8(b) shows that these exponents (squares) similarly decrease with increasing stress amplitude. Remarkably, aging exponents obtained by superposition of creep compliance curves (circles) appear to be identical to those found through mean-squared displacements after the stress is released. This indicates that the change in the aging exponent observed in nonlinear creep experiments is due to the evolving configuration of the glass, rather than the direct effect of stress on energy barriers, which would cease when the stress is removed.

It seems that the SGR model does produce rejuvenation in the relaxation times, but is the mechanically rejuvenated glass actually taken back in time by the application of stress? If this were the case, we would expect the relaxation after stress to proceed exactly like the younger, unstressed glass.

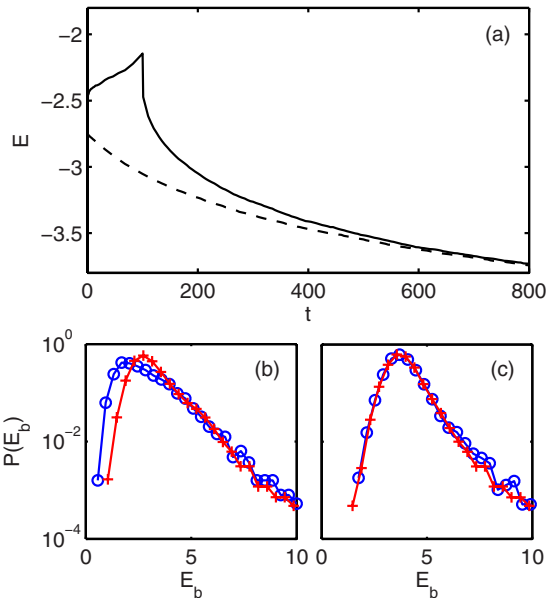

FIG. 9. (Color online) (a) Energy during a stress cycle and the subsequent recovery (solid line) compared to an unstressed glass (dashed). Samples are quenched from $x_l=\infty$ and aged for $t_w=100$ at $x=0.5$ before measurement. Stressed sample is loaded at $\sigma=0.7$ for $t=t_w$. (b), (c) The distribution of energy barriers of the unstressed sample (circles) and the stressed sample (+) at $t=125$ (b) and $t=800$ (c).

To investigate the relaxation behavior, a rejuvenated glass produced by a creep experiment with $\sigma=0.7$ (same data as Figs. 7 and 8) is relaxed after the stress cycle and compared to a sample aged without load. In Fig. 9(a) we see that the aging progresses much more rapidly after the stress cycle, and asymptotically approaches the energy relaxation trajectory of the unstressed sample. We also show the distribution of energy barriers of the stressed and unstressed samples at two times during the relaxation: almost immediately after the stress cycle is complete [Fig. 9(b)], and after the mean energies have converged [Fig. 9(c)]. The distribution of energy barriers (and consequently relaxation times) is greatly modified by the stress, but similarly converges to that of the unstrained sample during relaxation. This is despite the fact that, in this sample, approximately 50% of the strain is irreversible, held mostly by the deepest traps.

This is the essence of the paradox pointed out by McKenna [7]: although the stressed glass has an apparently rejuvenated relaxation spectrum, the time it takes to reach equilibrium is unchanged. In the SGR model, this has a simple explanation. Every time a trap relaxes, it releases the strain it was holding. Therefore, at constant (zero) stress, each relaxation causes a decrease in the strain energy of the entire ensemble of particles. This leads to a return to the unstrained aging trajectory over a timescale similar to the decay of the correlation function. It is conceivable that in real glasses, interactions between relaxing elements similarly explain McKenna's observations.

IV. CONCLUSIONS

We have performed stochastic simulations of the SGR model for strain-controlled and stress-controlled loading

cycles in the glassy phase. Both types of loading induce changes to the mean energy of the glass corresponding to regimes of mechanical rejuvenation and overaging. Within the SGR model, rejuvenation is the predominant effect, while overaging is only observed at low strains, low temperatures, and high energy initial configurations. These results are in qualitative agreement with molecular dynamics simulations of a model polymer glass over a wide range of loading parameters.

In addition to changes in the energy of the glass, mechanical rejuvenation is often observed as a decrease in the aging dynamics. To this end, we have evaluated the aging exponent through the scaling of the creep compliance with wait time, in direct analogy with experiment. As previously remarked in Ref. [30], the creep compliance in the SGR model strictly obeys full aging ($\mu=1$), even at very high load. In contrast, experiments [2,4,16] and MD simulations [14] show that the aging exponent decreases with stress amplitude in the nonlinear creep regime. The physics of this phenomenon does not seem to be captured by the SGR model; instead, the dynamical effects of mechanical rejuvenation appear only after the stress cycle. Aging exponents found from the t_w scaling of correlation functions after unloading decrease with increased stress, in qualitative agreement with MD simulations. Reconciling the stress dependence of the aging exponent in the SGR model with experiment would be a fruitful topic for further development of the model, but may require a better understanding of the physics of mechanical rejuvenation at the molecular level.

Finally, we have explored the relaxation dynamics after a rejuvenating stress cycle. The SGR model exhibits the fundamental difficulty with the "rejuvenation" hypothesis. While the relaxation times after a stress cycle appear to be exactly identical to a younger glass, the aging trajectory gradually returns to the undeformed path when the stress is released [7]. In the SGR model, this effect is due to collective strain relaxation which occurs after each hopping event. Identifying the effects of structural relaxations on the rejuvenated state may similarly provide insight to this effect in real glasses.

ACKNOWLEDGMENTS

We thank the National Sciences and Engineering Research Council of Canada (NSERC) and the Canadian Foundation for Innovation (CFI) for financial support.

[1] C. A. Angell, K. L. Ngai, G. B. McKenna, P. F. McMillan, and S. W. Martin, J. Appl. Phys. **88**, 3113 (2000).
[2] L. C. E. Struik, *Physical Aging in Amorphous Polymers and Other Materials* (Elsevier, Amsterdam, 1978).
[3] J. M. Hutchinson, Prog. Polym. Sci. **20**, 703 (1995).
[4] M. Cloitre, R. Borrega, and L. Leibler, Phys. Rev. Lett. **85**, 4819 (2000).
[5] D. Bonn, S. Tanase, B. Abou, H. Tanaka, and J. Meunier, Phys. Rev. Lett. **89**, 015701 (2002).
[6] J. J. Martinez-Vega, H. Trumel, and J. L. Gacougnolle, Polymer **43**, 4979 (2002).
[7] G. B. McKenna, J. Phys.: Condens. Matter **15**, S737 (2003).
[8] V. Viasnoff and F. Lequeux, Phys. Rev. Lett. **89**, 065701 (2002).
[9] H. Montes, V. Viasnoff, S. Juring, and F. Lequeux, Faraday Discuss. **123**, 253 (2003).
[10] D. J. Lacks and M. J. Osborne, Phys. Rev. Lett. **93**, 255501 (2004).
[11] M. Utz, P. G. Debenedetti, and F. H. Stillinger, Phys. Rev. Lett. **84**, 1471 (2000).
[12] A. V. Lyulin and M. A. J. Michels, Phys. Rev. Lett. **99**, 085504 (2007).
[13] J. Rottler and M. O. Robbins, Phys. Rev. Lett. **95**, 225504 (2005).
[14] M. Warren and J. Rottler, Phys. Rev. E **76**, 031802 (2007).
[15] K. Chen and K. S. Schweizer, Phys. Rev. Lett. **98**, 167802 (2007).
[16] A. Lee and G. B. McKenna, Polymer **31**, 423 (1990).
[17] H.-N. Lee, K. Paeng, S. F. Swallen, and M. D. Ediger, J. Chem. Phys. **128**, 134902 (2008).
[18] P. Bursac, G. Lenormand, B. Fabry, M. Oliver, D. A. Weitz, V. Viasnoff, J. P. Butler, and J. J. Fredberg, Nature Mater. **4**, 557 (2005).
[19] B. A. Isner and D. J. Lacks, Phys. Rev. Lett. **96**, 025506 (2006).
[20] D. M. Colucci, P. A. O'Connell, and G. B. McKenna, Polym. Eng. Sci. **37**, 1469 (1997).
[21] P. Sollich, F. Lequeux, P. Hebraud, and M. E. Cates, Phys. Rev. Lett. **78**, 2020 (1997).
[22] R. E. Courtland and E. R. Weeks, J. Phys.: Condens. Matter **15**, S359 (2003).
[23] K. Vollmayr-Lee and E. A. Baker, Europhys. Lett. **76**, 1130 (2006).
[24] P. Schall, D. A. Weitz, and F. Spaepen, Science **318**, 1895 (2007).
[25] C. Monthus and J. P. Bouchaud, J. Phys. A **29**, 3847 (1996).
[26] A. B. Bortz, M. H. Kalos, and J. L. Lebowitz, J. Comput. Phys. **17**, 10 (1975).
[27] K. Kremer and G. S. Grest, J. Chem. Phys. **92**, 5057 (1990).
[28] J. Rottler and M. O. Robbins, Phys. Rev. E **64**, 051801 (2001).
[29] R. A. Riggleman, K. S. Schweizer, and J. J. de Pablo, Macromolecules (to be published).
[30] S. M. Fielding, P. Sollich, and M. E. Cates, J. Rheol. **44**, 329 (2000).